Myoferlin Depletion in MDA-MB-231 Breast Cancer Cells Reduces Autocrine TGF-β1 Production

Victoria Barnhouse

Department of Biomedical Engineering

The Ohio State University

2017

Thesis Committee:

Dr. Jennifer Leight, Advisor

Dr. Douglas Kniss, Co-Advisor

Dr. Samir Ghadiali

Presented in Partial Fulfillment of the Requirements for Graduation with Honors Research Distinction in the Department of Biomedical Engineering at The Ohio State University

Abstract

Breast cancer is the second leading cause of cancer mortality in women, and metastatic disease is responsible for the majority of deaths. Epithelial cells within a tumor can undergo an epithelial-mesenchymal transition (EMT), enabling the cells to break free from the primary tumor and invade surrounding tissues. Recently, myoferlin (MYOF), a protein involved in cell membrane functions, was found to be overexpressed in the breast cancer cell line MDA-MB-231, and knocking down MYOF in these cells reduces invasion and reverts the cells to a more epithelial phenotype. However, it is unknown why knocking out MYOF leads to the reversal of EMT, and whether this change is permanent. Transforming growth factor β1 (TGF-β1) misregulation has been shown previously to contribute to the progression of cancer via EMT, and is known to be a potent stimulus of the process. To examine if the MYOF knockdown (KD) cells are capable of undergoing EMT, they were treated with TGF-β1. After treatment, their morphology converted to a more mesenchymal appearance. Therefore, we hypothesized that the knockdown of MYOF causes a decrease in autocrine TGF-β1 production, reversing EMT. Using an enzyme linked immunosorbent assay (ELISA), TGF-β1 levels were shown to have a 20% decrease in MYOF KD cells compared to control cells. Similarly, qRT-PCR of TGF-β1 showed about a 30% decrease in the mRNA expression levels in MYOF KD cells. Western blot was used to confirm the phenotypical change in TGF-β1 treated MYOF KD cells by comparing levels of specific markers present in epithelial and mesenchymal cells. Western blot of vimentin, a common mesenchymal marker, increased to a level similar to the MDA-MB-231 control cells after TGF-β1 treatment; E-cadherin, which is characteristic of epithelial cells, showed a significant decrease in expression. These findings confirm the EMT of MYOF KD cells after treatment. Studies on the effect of TGF-β1 on cell migration revealed a decrease in directionality, further supporting

the occurrence of EMT. These results indicate the importance of TGF-β1 in EMT of breast cancer cells, and gaining a better understanding of factors related to EMT can aid in the development of better and more specific treatment methods.

Acknowledgements

I would like to take a moment and thank all the people who contributed to making this work possible by helping me along the way.

First of all, I would like to thank my advisor, Dr. Jennifer Leight, for her support, motivation, and encouragement. Without her guidance and example, I would not be the researcher I am today, ready to take on the next step of my career with grad school. She allowed me the room to be independent, while always being there to help me when I needed it. Her mentorship was a contributing factor in my decision to pursue a PhD, and for that I am extremely thankful.

Secondly, I would like to thank all the past and present members of the Leight Lab, especially Kathryn, Jess, Ameya, Caitlin, and Abdul. Kathryn and I joined the lab at the same time, and she constantly inspired me with her enthusiasm and dedication. Jess has been a resource throughout my time in the lab, someone I could go to for technical advice or help with an experiment. She also was my partner on this project, and I would not have been able to accomplish nearly this many experiments without her help. Ameya, Caitlin, and Abdul have been another source of advice, whether through help with experiments or advice as I applied to grad school, all of them helped me along the way.

Lastly, I would like to thank my friends and family for their unwavering support. I am lucky enough to have parents who were able to help me pay for school, which allowed me to be able to spend hours in the lab. They also encouraged me to pursue what I love, and enjoy hearing about my research. Kelsey Watts has also been there for me through it all, as we both went through research and applying to grad school. She was always there to proofread my writing, and understand what I was going through.

Table of Contents

List of Tables

List of Figures

Chapter 1 Introduction

Breast cancer is the second leading cause of cancer mortality in women, with metastatic rather than localized disease leading to the majority of deaths. In the United States, the 5 year survival rate for women diagnosed with breast cancer is 99% for localized disease, 85% for regional disease, and 26% for distant disease ("Breast Cancer Facts & Figures | American Cancer Society" 2017). Epithelial-mesenchymal transition (EMT) is a process that can contribute to the metastasis of cancer cells, involving epithelial cells losing their cell-cell adhesions and gaining motility, allowing them to break away from the primary tumor and invade the surrounding tissue, infiltrate the blood vessels, and form a secondary tumor at another location in the body. By studying what leads to this transition in cancer cells, potential targets for more specialized therapeutic methods can be identified. The protein myoferlin (MYOF) was previously discovered to be overexpressed in invasive breast cancer lines (Li et al. 2012). After knocking down MYOF in the invasive breast cancer cell line MDA-MB-231, the cells exhibited a change to an epithelial phenotype, or a mesenchymal-epithelial transition (MET). It was unclear, however, why knocking down MYOF led to this MET, and if the change would permanently alter part of the mechanism of EMT, preventing it from occurring. In order for EMT to occur, cells must sense a stimulus and subsequently undergo a series of biochemical changes leading to the mesenchymal phenotype. In this study, we seek to discover what aspect of EMT knockdown of myoferlin is altering, the mechanism or the stimulus. We hypothesized that myoferlin depletion leads to a reduction in transforming growth factor β1 (TGF-β1) production, resulting in MET. To determine if MDA-MB-231 MYOF knockdown (KD) cells were able to undergo EMT, the cells were treated with exogenous TGF-β1, a known cause of EMT in many cell types. This resulted in a both morphological and phenotypical changes of the MDA-MB-231 MYOF KD cells to

become mesenchymal, based on western blot of EMT markers. Autocrine TGF-β1 concentrations were directly measured using an enzyme linked immunosorbent assay (ELISA), along with mRNA expression using qRT-PCR. Further studies on the effect of TGF-β1 treatment on migration were also performed, to validate that the phenotypical change altered cell behaviors, such as migration and invasion, as well.

Chapter 2 Background

2.1 Epithelial-Mesenchymal Transition

Epithelial-mesenchymal transition (EMT) is a process which allows a polarized epithelial cell to undergo biochemical changes enabling it to assume a mesenchymal phenotype (Kalluri and Weinberg 2009). There are multiple types of EMT, classified based on the biological context in which they occur. The first is type 1 EMT, which occurs during embryogenesis and is important for normal development. The major examples of EMT in embryogenesis include mesoderm, neural crest, and cardiac valve formation (Yang and Weinberg 2008). There are also cases during development where EMT is not an irreversible process permanently forming mesenchymal cells, but rather that the cells undergo a mesenchymal-epithelial transition (MET) reverting to an epithelial state (Davies 1996). Type 2 EMT occurs during tissue regeneration and organ fibrosis, as a response to inflammatory injury. The last type of EMT, type 3, is associated with cancer progression and metastasis.

In order for cancer cells to break away from the primary tumor and neighboring cells, they must lose their cell-cell adhesions and gain motility, which is believed to occur through a type 3 EMT. EMT has been found to be regulated through many controls at the transcriptional, post-transcriptional, translational, and post-translational levels (Craene and Berx 2013).

A variety of transcriptional factors are known to repress E-cadherin and other cell junction proteins. Loss of E-cadherin is associated with cancer progression and poor prognosis, since it is a cell adhesion molecule and key part of an epithelial state. In many types of carcinoma, the tumor loses E-cadherin expression early during development, and thus the cells are in a permanent mesenchymal phenotype, or an irreversible EMT (Guilford et al. 1998). This

is not necessarily the case, however, since carcinoma cells are believed to activate the EMT process to invade and travel to distant organs, after which they revert via a MET and form secondary tumors. While the EMT process in embryonic development is well-defined, in carcinoma progression it is difficult to understand, since cells can undergo partial EMT to their advantage as well. The transcriptional factors Snail, Slug, and Twist have been found to be important in the regulation of the process of EMT, both in normal development and cancer progression (Hugo et al. 2007). The Snail family, which includes Slug, represses the transcription of the adherens junction E-cadherin by binding an element in the E-cadherin promoter, which is also the mechanism by which Twist works (Hugo et al. 2007; Martin et al. 2005). Twist inhibits oncogene and p53-dependent cell death, thus making it an antiapoptotic factor, and is also known to trigger EMT (Martin et al. 2005).

Non-coding RNAs, including microRNAs (miRNAs) have recently been found to be important in the regulation of EMT. The miR-200 family is associated with epithelial differentiation, and the feedback with an EMT transcription factor controls both EMT and MET (Korpal et al. 2008). Additionally, the miR-34 family controls Snail-dependent EMT (Kim et al. 2011).

The transforming growth factor-β (TGF-β) family of proteins is known to be important in both normal development and cancer progression EMT. Activation of the TGF-β signal pathway in later stages of tumor progression was shown to lead to EMT, allowing the cells to spread to distant organs (Janda et al. 2002). TGF-β has also been shown to induce Snail and Slug, which then would lead to lower expression of E-cadherin.

The relevance of EMT in clinical settings is often questioned due to the difficulty in identifying markers of EMT from clinical samples. This is likely due to the transient nature of

EMT changes, along with the fact that it may occur in only a small number of cells at the invasive edge of the tumor, which has been supported by clinical data. Most human cancers have partial EMT features, and express both markers of epithelial and mesenchymal cells in vivo (Craene and Berx 2013).

Similarly, in a study on pancreatic ductal adenocarcinoma, EMT regulators Snail and Twist1 were knocked out to study if this reduces the invasion and metastasis of cancer cells in mice. It was found that the cancer cells were still able to proliferate and metastasize. However, knocking out Snail and Twist1 did make the tumors more susceptible to the gemcitabine drug, where normally EMT is associated with resistance to this drug. Tumor progression was able to be suppressed and survival was increased in the knockout mice (Zheng et al. 2015). Another study on lung metastasis in breast cancer also found that EMT was not required for metastasis to occur, in a mouse model where EMT was suppressed. The study also found that cells that had undergone EMT were able to resist chemotherapeutics both in vitro and in vivo (Fischer et al. 2015). Thus, although not necessary for metastasis, EMT is responsible for drug resistance and targeting this process could help lead to improved patient outcomes.

2.2 Myoferlin

Myoferlin (MYOF) is a protein of the ferlin family, which are important in cell membrane functions such as fusion, repair, and endocytosis. It was shown to be critical for endocytosis in epithelial cells, after disrupting the gene resulted in decreased endocytosis (Bernatchez et al. 2009). Additionally, a study on pancreatic cancer showed MYOF to be critical for the exocytosis of VEGF, as staining for the protein revealed an aggregation at the cell membrane after MYOF silencing. They also found significantly lower concentrations of VEGF in the conditioned media of the myoferlin silenced cells, but no significant difference in the

mRNA expression, leading to the conclusion that myoferlin silencing regulates the exocytosis of VEGF. Silencing also led to decreased tumor volume, due to the reduction of blood vessels within the tumor (Fahmy et al. 2016).

MYOF was previously found to be overexpressed in highly invasive breast cancer cell lines compared to normal breast tissue. To study how this protein affected the invasive capacity of MDA-MB-231 cells, the gene for MYOF was knocked down (Li et al. 2012). After myoferlin depletion, the MDA-MB-231 cells appeared to have an epithelial phenotype (Fig 2-1). This observation was confirmed by western blot to analyze protein expression, which showed a down-regulation of the mesenchymal markers fibronectin and vimentin, and corresponding up-regulation of the epithelial marker E-cadherin. Along with a phenotypical change, the study reported a decrease in invasion of the MDA-MB-231 myoferlin knockdown (MYOF KD) cells through both matrigel and collagen type I.

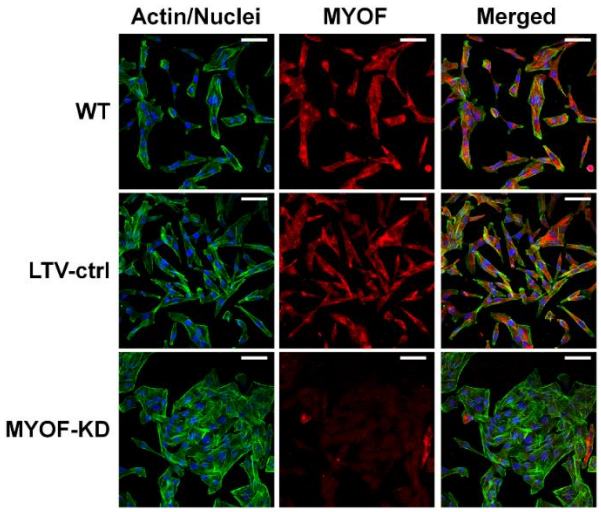

Figure 2-1: Effect of Myoferlin Depletion on MDA-MB-231 Cells. Immunofluorescent images showing the morphology of MDA-MB-231 wild type (WT), lentiviral control (LTV-ctrl), and myoferlin knockdown (MYOF-KD). The MYOF-KD cells appear more cobblestone in shape characteristic of epithelial cells, while the WT and LTV-ctrl cells have the spindle shape characteristic of mesenchymal cells (Li et al. 2012).

In addition to the change in phenotype and invasion, MYOF depletion resulted in a change in migration patterns to collective migration, with decreased velocity and increased directionality of movement (Volakis et al. 2014). Additionally, MYOF depleted cells displayed

enhanced cell-substrate adhesion and spreading, more than 2 times greater than control cells (Fig. 2-2). In vivo studies in mice found that MYOF KD cells formed smaller, smooth edged tumors that did not appear to invade the surrounding tissue, showing that the depletion of myoferlin is able to prevent invasion. Furthermore, a similar study on mouse Lewis lung carcinoma found that myoferlin knockout in vivo in mice reduced tumor burden and growth (Fig. 2-3) (Leung et al. 2013). Analysis of the expression of proteins that control cell-matrix adhesions, including focal adhesion kinase (FAK) and paxillin (PAX), found cell adhesions in MYOF KD cells to be larger and more elongated, with increased localization at the cell periphery (Blackstone et al. 2015). These results indicate both by cell structure and activity that MDA-MB-231 MYOF KD cells underwent MET.

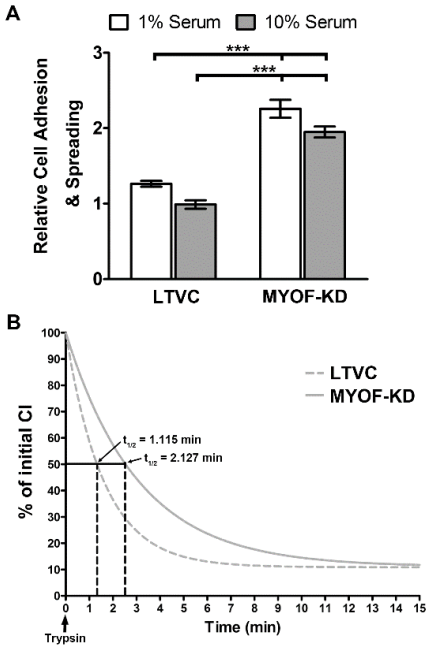

Figure 2-2: MYOF knockdown MDA-MB-231 cells have enhanced cell-substrate adhesion. A. Relative cell adhesion and spreading was calculated and normalized to wild type cells (data not shown). The MYOF knockdown cells were found to have cell adhesion and spreading two times greater than the lentiviral control (LTVC) cells. **B**. Cell detachment after addition of trypsin. The release time of MYOF knockdown cells was two times greater than LTVC cells (Volakis et al. 2014).

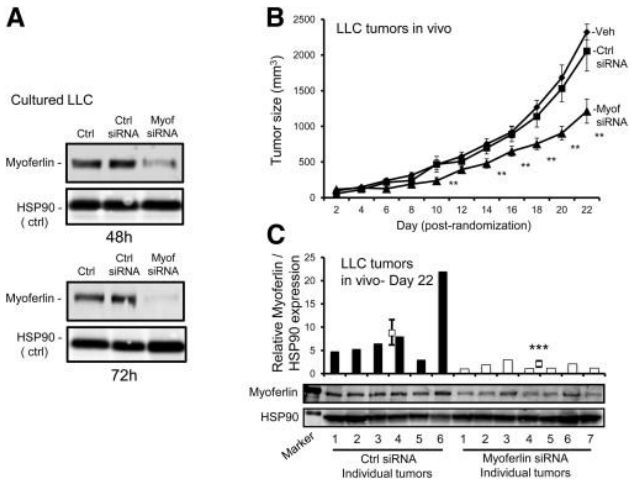

Figure 2-3: Study of the growth of tumors in mice after knockdown of myoferlin. A. Lewis lung carcinoma cells (LLC) were treated with vehicle, control siRNA, or myoferlin siRNA for 48 and 72 hours, after which proteins were isolated to verify knockdown was successful. B. Mice were injected with cells of the various conditions, and myoferlin knockdown was found to significantly decrease tumor burden. C. After mice were euthanized, tumors were isolated, and proteins were blotted to observe myoferlin expression in the tumors (Leung et al. 2013).

2.3 Transforming Growth Factor β

Transforming growth factor β (TGF-β) is a superfamily of growth factors, containing over 30 members, including bone morphogenetic proteins (BMPs), growth and differentiation factors (GDFs), Activins, and Nodal in addition to TGF-βs, which are important for development and homeostasis, regulating many cellular functions including growth, adhesion, migration, apoptosis, and differentiation (Wu and Hill 2009). During early stages of tumor development, TGF-β has been shown to act as a tumor suppressor, inducing apoptosis in normal epithelial cells. However, in later stages of tumor development, TGF-β aids in tumor progression, by enhancing migration, invasion, survival, and EMT. This switch was found to be partially regulated by matrix rigidity, with decreased rigidity leading to apoptosis, and increased rigidity leading to EMT (Leight et al. 2012).

Extensive research has focused on the signaling pathways of TGF-β, and how they regulate EMT. There are three isoforms of TGF-β, named TGF-β1, TGF-β2, and TGF-β3. They function by binding type I, type II, and type III receptors (TβRI, TβRII and TβRIII). Binding of

TGF-β to TβRII recruits and phosphorylates TβRI (Lei et al. 2002). Activated TβRI then phosphorylate Smad2 and Smad3 proteins, two of which then combine with Smad4 and translocate into the nucleus, where the complex can regulate gene expression. Some of the transcriptional targets of TGF-β signaling include Snail/Slug, ZEB1/2 and Twist, all of which regulate EMT. TGF-β signaling also activates other pathways, including PI3K/Akt, Erk, and Rho-GTPases. The PI3K/Akt/mTOR pathway promotes increased protein synthesis, motility, and cell invasion (Katsuno, Lamouille, and Derynck 2013). The protein kinase mTOR complex 2 directs the cytoskeletal reorganization during EMT. Small GTPases control cytoskeletal regulation as well, and are controlled by TGF-β signaling by transcriptional methods as well as post-transcriptional regulation. This signaling leads to proteasomal degradation, resulting in decreased stiffness and remodeling of the cytoskeletal response to enhance invasion (Moustakas and Heldin 2016). A summary of TGF-β signaling pathways can be found in Figure 2-4.

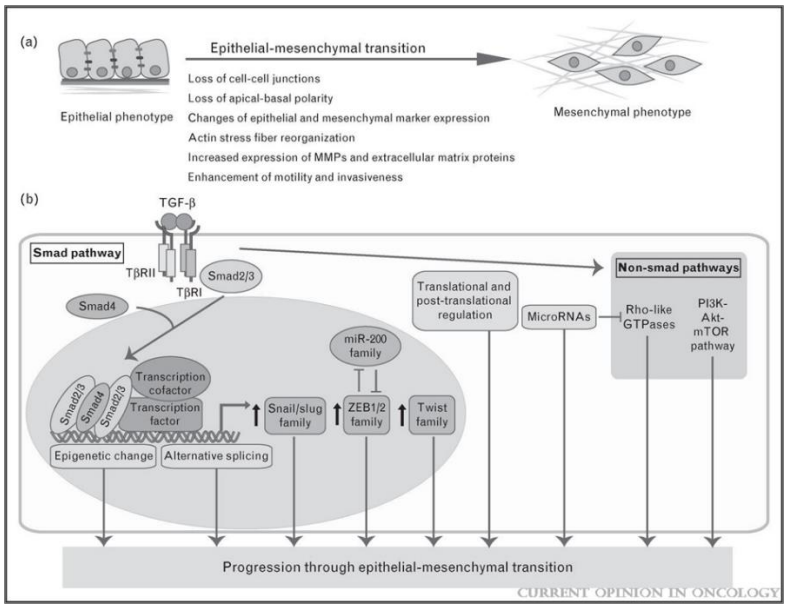

Figure 2-4: Transforming Growth Factor Beta Regulation of Epithelial-Mesenchymal Transition. a) Epithelial-mesenchymal transition occurs when epithelial cells lose their cell-cell adhesions and apical-basal polarity, and gain properties of mesenchymal cells including enhanced mobility and invasion, characterized by the reorganization of the actin cytoskeleton, increased expression of matrix metalloproteinases (MMPs) and extracellular matrix proteins. b) TGF-β induces EMT through both the Smad pathway and non-Smad pathways. The Smad2/3 and Smad 4 complex translocates into the nucleus and regulates the transcription of target genes. Smad

signaling increases the expression of Snail/Slug, Zeb1/2 and Twist, which are responsible for repressing epithelial markers and activating mesenchymal markers. The PI3K-Akt-mTOR pathway and GTPases are also activated, increasing motility and invasion and changing actin organization (Katsuno, Lamouille, and Derynck 2013).

TGF-β was found to be critical for the growth and survival of MDA-MB-231 cells. Upon sequestering active TGF-β1 and TGF-β2 using the expression of a soluble TGF-β type III receptor, sRIII, Smad2 phosphorylation was found to be decreased compared to the control cells, and it was further found that sRIII expression antagonized autocrine TGF-β activity. Additionally, when control MDA-MB-231 cells were treated with a recombinant sRIII or neutralizing antibody specific to TGF-β1 or TGF-β2, their growth was inhibited. A neutralizing antibody binds directly to the TGF-β protein, preventing it from activating the signaling pathway. When comparing cell death, it was found that sRIII clones had significantly more apoptosis than control cells (Lei et al. 2002). Similarly, another study inhibited TGF-β using both a neutralizing antibody (1D11) and a chemical inhibitor of the type I and type II receptors (LY2109761) in MDA-MB-231 cells. It was found that blocking TGF-β inhibited the phosphorylation of Smads 2 and 3. In vivo, treatment with the inhibitors reduced the burden of metastases, indicating the importance of TGF-β for the growth and metastasis of MDA-MB-231 cells (Ganapathy et al. 2010; Liu et al. 2012).

Blocking TGF-β was also found to alter the vasculature of tumors and improve the perfusion of vessels within the tumor, allowing for the distribution of drugs into the tumors. The extracellular matrix around the tumor was altered as well, with significantly decreased collagen I content, resulting in a less dense matrix that allowed better penetration of drug into the tumor tissues (Liu et al. 2012). These results indicate how targeting TGF-β may help lead to better patient outcomes by enhancing the susceptibility of tumors to traditional treatment methods.

2.4 The 3D Microenvironment and Tumor Behavior

Factors related to the 3D environment of tumor cells, including the components of the extracellular matrix (ECM) and mechanical stiffness of the surrounding tissue, are important regulators of tumor progression. Part of the process of metastasis involves the ability of the cancer cells to degrade the basement membrane and ECM to migrate and spread to other tissues. Matrix metalloproteinases (MMPs) are enzymes that degrade components of the ECM, including collagen and fibronectin. Under normal conditions, MMPs and their specific tissue inhibitors of MMPs (TIMPs) have a tightly controlled balance that maintains the homeostasis of ECM degradation. High levels of certain MMPs have previously been shown to predict poor prognosis in cancer (Têtu et al. 2006). In breast cancer, MMP-2 and MMP-9, the gelatinases, are implicated for their specific degradation of collagen type IV, which is an abundant basement membrane protein in that tissue. MMP-14 is also implicated in breast cancer progression, since it is involved in MMP-2 activation and is important for invasion and migration (Gomes et al. 2012; Têtu et al. 2006). MMP-14 is a membrane bound MMP which localizes to structures called invadopodia in the membrane structure. Its direct degradation of the matrix enables it to promote cell invasion (Itoh 2015). In a study looking at the downregulation of MMP-14 in 231 cells, it was found that the growth of the primary tumor was not affected, however, the number of metastases to the lungs was significantly reduced (Perentes et al. 2011). This indicates the important role of MMP-14 in the metastasis of cancer cells.

In a clinical study on the correlation between tissue stiffness and breast cancer prognosis, it was found that higher histologic grade was associated with higher mean stiffness (Evans et al. 2012). Tumor stroma is characterized by remodeling and stiffening of the ECM, and the stiffness enhances the cell growth, survival, and migration of cancer cells. A study in rats found an

incremental stiffening of the mammary gland as it transitioned from normal, to premalignant, to invasive cancer, along with the adjacent stromal tissue becoming stiffer than normal as well. The increase in stiffness was associated with increased collagen crosslinking (Levental et al. 2009). In a study in mice, normal mammary tissue was found to have a stiffness of ~0.2 kPa, while tumor samples ranged from ~3-5 kPa, illustrating the dramatic changes in elastic modulus after tumor formation (Paszek et al. 2005).

Since cancer cells are in a 3D rather than 2D environment in vivo, studying factors such as mechanical environment and ECM composition is best done either in an in vitro 3D model or an in vivo animal model. 3D in vitro models offer a useful alternative to the complexity of whole organism animal models, and offer the ability to tune the characteristics of the environment the cells are tested in. There are numerous approaches to 3D culture, including natural scaffolds, synthetic scaffolds, and cell excreted ECM (Nyga, Cheema, and Loizidou 2011). Synthetic hydrogels can be engineered to have specific mechanical and chemical properties to mimic certain properties of the native ECM. Using these approaches allows for the study of the effects of both the mechanical environment combined with other factors that may contribute to the behavior of cells, such as ECM components present or soluble factors.

Chapter 3 Methodology

3.1 Cell Culture

MDA-MB-231 breast cancer cells with a stable lenti-viral knockdown of MYOF (MDA-MB-231 MYOF KD) and lenti-viral control cells (MDA-MB-231 LTV CNTL) received from the Kniss lab were cultured in high glucose Dulbecco's modified eagle medium (HG DMEM) supplemented with 10% fetal bovine serum (FBS) (VWR), 1% L-glutamine (Life Tech) and 1% penicillin-streptomyosin (Life Tech) for normal growth (Li et al. 2012). For experiments, cells were cultured in high glucose DMEM supplemented with 1% L-glutamine (Life Tech) and 1% pen-strep (Life Tech). Insulin-Transferrin-Selenium-G (ITS) supplement (Invitrogen) was added for Western Blot, proliferation and metabolism studies. For migration assays, 10% charcoal stripped FBS was added to the experimental media.

3.2 TGF-β1 Treatment

Recombinant Human TGF-β1 (PeproTech) was used at a concentration of 2 ng/mL, and dissolved in 4 mM HCL with 0.1% bovine serum albumin (BSA) (Sigma-Aldrich). Cells were plated in growth medium and after 24 hours, were switched to experimental media supplemented with either TGF-β1 or vehicle control and cultured for 48 hours.

3.3 ELISA

Cells were plated at a density of $2.0x10^4$ cells/cm^2 with normal growth media in six-well culture plates and switched to experimental media after 24 hours. Cell culture supernatant was collected after 48 hours of culture in experimental media. Samples were assayed directly after collection. A Human TGF-β1 Quantikine ELISA kit (R&D Systems) was used to quantify the amount of TGF-β1 made by each cell type. The kit was used according to the manufacturer's

protocol, and samples were activated prior to running the assay using a sample activation kit (R&D Systems). Absorbance values were measured at 450 nm and 540 nm with the Spectra Max M2 plate reader (Molecular Devices).

3.4 Quantitative RT-PCR

Cells were plated at a density of $1x10^7$ cells/cm^2 overnight (16 hrs) then starved for 2 hours in serum-free media. Cells were then treated with TGF-β1 or vehicle control for 2 hours prior to lysis. RNA isolation was performed using the RNeasy Mini Kit (Qiagen) according to the manufacturer's protocol, using the Qiashredder columns (Qiagen) to homogenize the samples. The RNA was converted to complementary DNA using iScript (Bio-Rad) in a 20 µL reaction performed using a thermal cycler (BioRad) with 1 µg of RNA. The mRNA expression was analyzed using qRT-PCR in triplicate with SYBR Green reagent (Fisher Scientific) at 1:2 in each well, with cDNA at 1:100. The mRNA fold changes were determined using the ΔΔCT method normalized to the 18S endogenous control. The primer sequences are listed in Table 3-1.

Table 3-1: Primer Sequences. Sequences used for quantitative RT-PCR**.**

Primer	Forward Sequence	Reverse Sequence
TGF-β1 (Yin et al. 2016)	GGCGATACCTCAGCAACCG	AAGGCGAAAGCCCTCAAT
Slug (Dhasarathy, Kajita, and Wade 2007)	AGATGCATATTCGGACCCAC	CCTCATGTTTGTGCAGGAGA
Snail (Medici, Hay, and Olsen 2008)	ACCACTATGCCGCGCTCTT	GGTCGTAGGGCTGCTGGAA
Twist1 (Elias et al. 2005)	GAGTCCGCAGTCTTACGAGG	CTGCCCGTCTGGGAATCACT

3.5 Western Blot

Cells at a density of $2x10^4$ cells/cm^2 were plated in six-well culture dishes with growth media for 24 hours and then switched to experimental media with TGF-β1 or vehicle control. After 48 hours, plates were rinsed in ice-cold PBS and lysed for 10 minutes on ice using radioimmunoprecipitation assay (RIPA) buffer (Life Tech) with Halt protease and phosphatase inhibitor cocktails (Fisher Sci) at 1:100. Samples were centrifuged at 12,000 rpm for 15 minutes after lysis, and the supernatant was transferred to fresh pre-chilled tubes. Protein concentrations were determined using a μBCA protein assay (Thermo Fisher). Equal amounts of protein (30 μg) were separated using sodium dodecyl sulfate polyacrylamide gel electrophoresis (SDS-PAGE) with a 12% Bis-Tris Plus Gel (Invitrogen) and transferred to a polyvinylidene difluoride (PVDF) membrane (Fisher Sci). The membrane was blocked with Tris-buffered saline with Tween20 (TBST) (5% BSA (Sigma Aldrich) in TBS + 0.05% Tween20 (Sigma Aldrich)) for 1 hour at room temperature. Membranes were probed with primary antibodies: mouse monoclonal E-cadherin (Cell Signaling Technologies), mouse monoclonal vimentin (Fisher Scientific), and the loading control mouse monoclonal glyceraldehyde 3-phosphate dehydrogenase (GAPDH) (Fisher Scientific), diluted in blocking solution. After rinsing, membrane sections were incubated with horseradish peroxidase-conjugated secondary antibodies (Thermo Fisher) for 1 hour at room temperature and rinsed again 3 times. SuperSignal West® femto (for E-cadherin) and pico (for vimentin and GAPDH) chemiluminescent substrates (Thermo Fisher) were added to the appropriate membrane sections for 5 minutes prior to imaging. Membranes were visualized using the LiCor Odyssey Fc Imaging System, then quantified using ImageJ (NIH, Imagej).

3.6 Cell Proliferation and Metabolism

For proliferation studies, cells at a density of $2x10^4$ cells/cm^2 were plated in six-well culture dishes, and following 48 hours of culture in experimental media supplemented with either TGF-β1 or vehicle control, plates were rinsed with PBS and frozen at -70°C for at least 24 hours prior to assay. The CyQUANT Cell Proliferation assay kit (Invitrogen) was used according to the manufacturer's protocol to determine the relative cell number. To determine cell metabolism, AlamarBlue cell viability reagent (Life Technologies) was added to each well at a 1:10 dilution for six hours prior to the 48 hour time point, then read using the Synergy HT plate reader (BioTek) at 540 nm excitation/590 nm emission.

3.7 Migration

Migration studies were performed using Ibidi® chambers and live cell tracking of cell movement. Cells were seeded at $2x10^4$ cells per chamber, grown overnight in normal culture media, and then the cells were pretreated with or without TGF-β1 for 48 hours. After 48 hours, the Ibidi insert was removed, cells were washed to remove any non-adhered cells and experimental media was added to fill the well. An inverted fluorescence microscope (Olympus IX81) with live cell imaging chamber (Okolab) was used to record bright field images of cells every ten minutes over 24 hours. Time-lapse images thus collected were analyzed using image processing software ImageJ (NIH, Imagej) to track individual cell migration. Cell position data were then analyzed using MATLAB to determine cell migration parameters including accumulated distance, cell velocity, Euclidean distance and cell directionality. The code used for this analysis can be found in Appendix A.

3.8 Polyethylene Glycol (PEG) Hydrogels

A master mix of the components of the hydrogel was made with 3 mM (6 wt%) polyethylene glycol-norbornene (PEG-NB), MMP crosslinker (KCGPQGIWGQCK), 1 mM CRGDS, 2 mM photoinitiator LAP, and 0.25 mM fluorogenic peptide (Leight et al. 2013). The fluorogenic peptide contains a quencher and a fluorophore, and after cleavage is able to fluoresce for detection. The peptide used in this study is sensitive to cleavage by MMP 14. In order to alter the stiffness of the hydrogel, different PEG-NB types and crosslinking ratios were used, as outlined in Table 3-2. Cells were encapsulated by making a concentrated cell suspension in phosphate buffered saline (PBS) which was added to the master mix, for a final cell density of $4x10^6$ cells/mL. Fifty µL of the master mix and cell solution was pipetted into a rubber gasket with a 6 mm inner diameter on a thiolated coverslip, to covalently link the gel to the coverslip. The solutions were then exposed to 365 nm light for 3 min to crosslink the gel. After encapsulation, gels were incubated in 1% charcoal stripped serum HG DMEM for 24 hours, and a 0 hour fluorescence reading was taken as a background. Six hours prior to the end of the experiment, AlamarBlue cell viability reagent (Life Technologies) was added to each well at a 1:10 dilution. One hour prior to the final fluorescence reading, nucleic acid stain Hoechst (Invitrogen) was added to each well at a 1:2000 dilution. Fluorescence measurements were taken on the Spectra Max M2 plate reader (Molecular Devices) at 494 nm excitation (ex)/ 521 nm emission (em) for the fluorogenic peptide, 560 nm ex/ 590 nm em for AlamarBlue, and 350 nm ex/ 461 nm em for Hoechst. Prior to the fluorescence reading for Hoescht, media were removed from the wells and PBS was added to remove any Hoescht that was not bound to the nuclear DNA. Fluorescence values were normalized both to cell metabolism (AlamarBlue) and DNA

content (Hoechst) to obtain the relative MMP activity. Coverslips were thiolated as described previously (Carman et al. 2006).

Table 3-2: Experimental Setup of Gel Stiffness Experiments. Table of the PEG-NB used, along with the crosslinking ratio and corresponding Elastic Modulus for the gel stiffness experiments.

PEG-NB	Crosslinking Ratio	Elastic Modulus (kPa)
4 ARM 20K	1.0	0.753
8 ARM 40K	0.70	1.428
8 ARM 40K	0.85	2.599
8 ARM 40K	1.0	3.427
8 ARM 20K	0.70	2.577
8 ARM 20K	0.85	5.387
8 ARM 20K	1.0	6.211

3.9 Statistical Analysis

Data analysis for graphical representation and statistical results was performed using Prism version 7 (GraphPad). Error bars represent the standard deviation of the samples. For data sets with 3 or more groups, statistical analysis was performed using a two-way ANOVA followed by a Tukey's Multiple Comparison Test with an alpha level of 0.05. For data with two sets, an unpaired one-tailed t-test was conducted to determine significance, with an alpha level of 0.05. For the gel stiffness experiments, statistical analysis was performed using linear regression, to determine if the slopes and intercepts of the two data sets were significantly different, with a confidence interval of 95%.

Chapter 4 Results

4.1 Transforming Growth Factor-β1 Induced Epithelial-Mesenchymal Transition

MYOF knockdown results in a change in phenotype and morphology of the MDA-MB-231 cells from mesenchymal to epithelial (Li et al. 2012). It is not known, however, the mechanism leading to this change after MYOF depletion, or if the transition is reversible. In order to determine if the MYOF KD cells retained their ability to undergo EMT, they were treated with TGF-β1, since TGF-β1 is known to be a potent stimulus of EMT. After treatment with exogenous TGF-β1 for 48 hours, MYOF KD cells had a dramatic change in morphology, as visualized using light microscopy. Vehicle-treated MYOF KD cells exhibit the cobblestone-like morphology characteristic of epithelial cells, and vehicle-treated control cells have the elongated, spindly shape characteristic of mesenchymal cells. The MYOF KD cells treated with TGF-β1 appear more similar to the control cells, with a more elongated morphology, as seen in Figure 4-1. Additionally, treatment with TGF-β1 was not found to significantly alter the proliferation or metabolism of the cells (data in Appendix B).

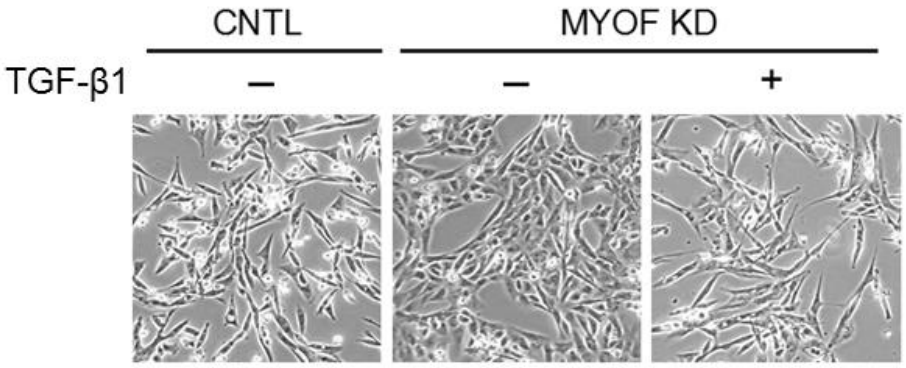

Figure 4-1: Effect of TGF-β1 on Myoferlin Depleted MDA-MB-231 Cells. Phase images of MDA-MB-231 MYOF KD cell morphology after treatment with TGF-β1.

In addition to changes in morphology, an EMT is also accompanied by changes in protein expression of epithelial and mesenchymal markers. Western blot for common markers of EMT

was performed and results are shown in Figure 4-2. Vimentin, a common marker of a mesenchymal phenotype, was found to be significantly upregulated in the MYOF KD cells, and closer to the levels of vimentin in the control cells. Similarly, E-cadherin, a cell adhesion protein and marker of an epithelial phenotype, was found to be significantly decreased in the MYOF KD cells. Control cells treated with TGF-β1 showed little change. The morphology change together with the phenotypic change shown by western blot indicates that the MYOF KD cells underwent an EMT after being treated with TGF-β1, and therefore retain their plasticity.

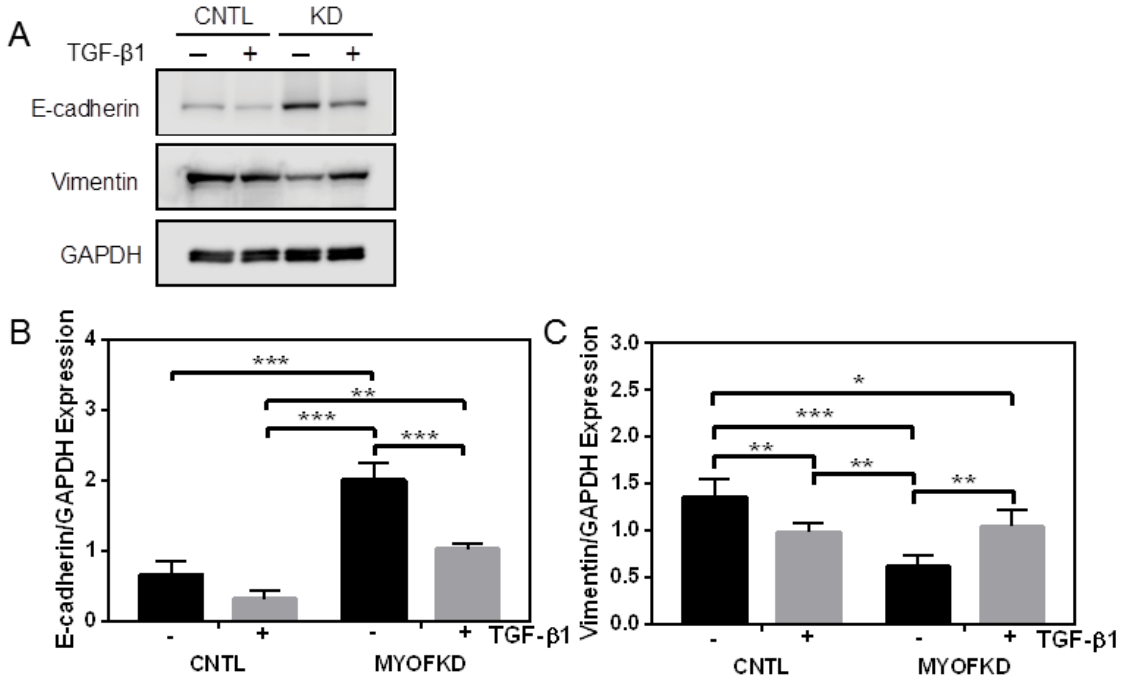

Figure 4-2: Western Blot of EMT Markers. A) Representative immunoblot of EMT markers vimentin and E-cadherin in MDA-MB-231 control (CNTL) and myoferlin knockdown (KD) after treatment with vehicle control or TGF-β1 for 48 hours. B) E-cadherin expression levels normalized to the loading control GAPDH. C) Vimentin expression levels normalized to the loading control GAPDH. n=3+SD, *p<0.05, **p<0.01, ***p<0.001

Further analysis of EMT was performed by determining the mRNA expression levels of transcription factors known to regulate EMT, Snail, Slug, and Twist, which repress E-cadherin. Both Snail and Slug were found to be significantly increased in MYOF KD cells upon treatment with TGF-β1, indicating that the MYOF KD cells were undergoing EMT as shown in Figure 4-3.

This result further supports the western blot data that an EMT has occurred in the MYOF KD cells, indicating that these cells are still capable of undergoing EMT after myoferlin depletion. Although average values of the vehicle control MYOF KD expression were lower than that of the control cells, this difference was not found to be significant. Furthermore, since Snail and Slug are both activated by TGF-β, an increase in expression following treatment in the control cells would be expected. Twist had high CT values, which prevented quantification, indicating that the MDA-MB-231 cells are expressing very low levels.

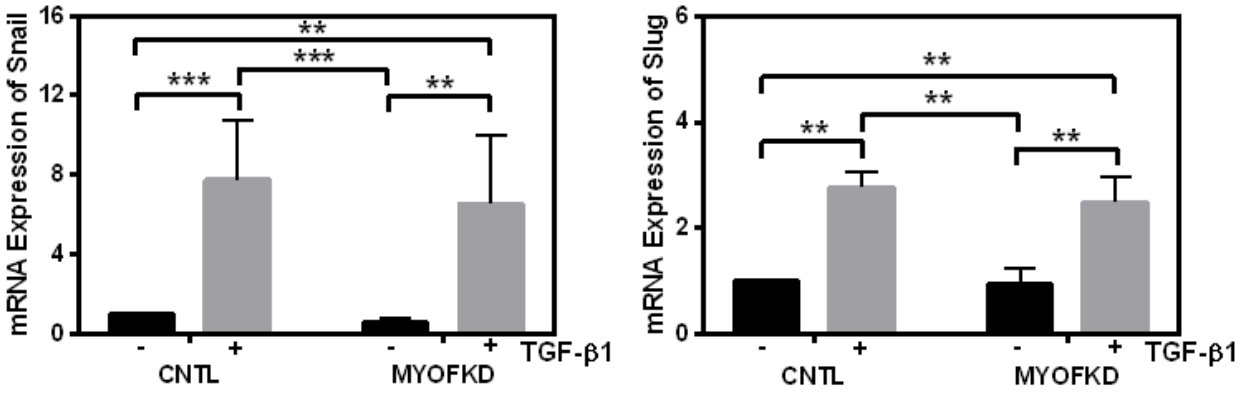

Figure 4-3: mRNA Expression of Snail and Slug Transcription Factors. Snail and Slug mRNA were significantly increased in the MYOF KD cells after treatment with TGF-β1. n=3+SD, *p<0.05, **p<0.01, ***p<0.001.

4.2 Effect of Myoferlin Depletion on Transforming Growth Factor-β1 Production

TGF-β1 is known to be an important regulator of EMT, due to its regulation of various transcriptional factors that influence the production of epithelial and mesenchymal markers. Additionally, it has previously been shown that MDA-MB-231 cells produce autocrine TGF-β1 (Lei et al. 2002). Since the addition of TGF-β1 induced an EMT in the MYOF KD cells, we hypothesized that the depletion of MYOF may result in a reduction in autocrine TGF-β1 production. In order to directly detect TGF-β1 levels made by the CNTL and MYOF KD cells, an ELISA was performed on the conditioned media of each cell type. The relative expression

levels were determined, and the MYOF KD cells were found to secrete approximately 20% less TGF-β1 than the control cells, with an average value of 0.77 +/- 0.052 when normalized to the control cells, as shown in Figure 4-4. The values were found to be statistically different, with a p-value of 0.024 using an unpaired one-tailed t-test. Therefore, the MYOF KD expression of TGF-β1 is significantly lower than that of the control cells.

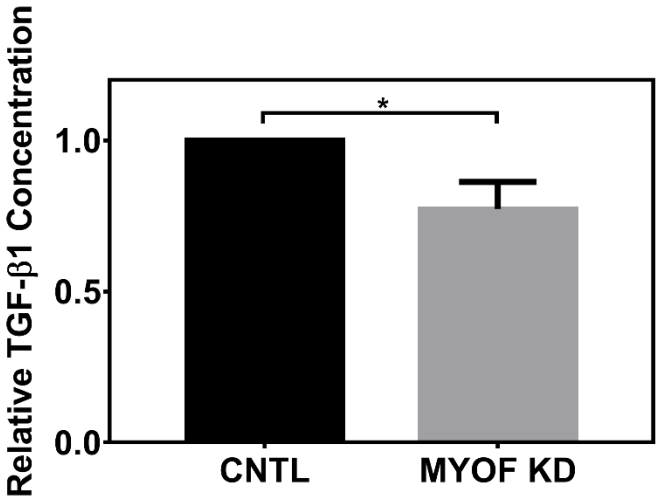

Figure 4-4: Relative TGF-β1 Concentration. An ELISA specific for TGF-β1 was used to quantify the relative concentration produced by the control and myoferlin depleted cells. n=3, *p<0.05.

MYOF could regulate the protein expression of TGF-β1 through a variety of pathways, such as secretion from the cell or transcriptionally. To investigate the latter, measurement of TGF-β1 mRNA expression was determined using quantitative RT-PCR. Similar to the ELISA results, TGF-β1 expression was found to be decreased by approximately 30% in the MYOF KD cells, with an average value of 0.71 +/- 0.108 when normalized to the control cells, as seen in Figure 4-5. However, the data sets were not found to have a statistical difference, with a p-value of 0.0558 using an unpaired one-tailed t-test. Although these reductions in production are small, it is possible there is a critical level of TGF-β1 needed for EMT to occur. It has been shown

previously that MDA-MB-231s produce TGF-β and that autocrine signaling is required for cell survival (Lei et al. 2002).

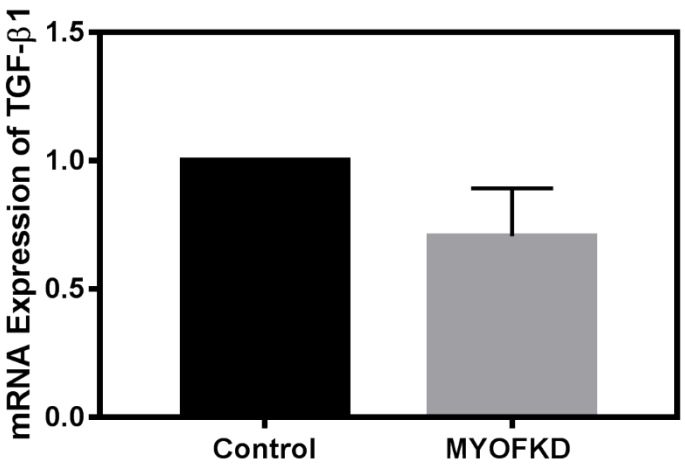

Figure 4-5: TGF-β1 mRNA Expression. Relative quantities of TGF-β1 mRNA were determined using quantitative RT-PCR. n=3, p=0.0558

4.3 Effect of Transforming Growth Factor β on Migration

MYOF depletion in MDA-MB-231s causes changes in cell migration. A previous study found MYOF KD cells to exhibit collective migration, rather than the single cell, random migration of the control cells, with decreased velocity and distance traveled, and increased directionality (Volakis et al. 2014). To determine if TGF-β1 treatment of the MYOF KD cells also affected cell migration, control and MYOF KD cells with or without TGF-β treatment were allowed to migrate for 24 hours and phase images were taken every ten minutes. The cells were first pretreated with or without TGF-β for 48 hours, to ensure the cells exhibited the EMT changes described above prior to the experiment. These images were then processed to analyze trends in migration patterns, the graphs of which are seen in Figure 4-6. Representative images of each condition before and after migration can also be seen in Figure 4-7.

Accumulated distance describes the total distance traveled by a cell, while Euclidean distance is the distance from the start point to the end point with a straight path between the points. Velocity is found from the distance traveled at each time point divided by the time between data points. Directionality indicates if the cell is preferentially moving in a certain direction, and is calculated by the Euclidean distance/accumulated distance. The trends in migration patterns follow the results seen previously, however most are not significant. After adding TGF-β1, there is a change in directionality, which is significantly decreased in the TGF-β1 treated MYOF KD cells, to a value similar to that of the control cells. This indicates a change from the collective migration of the knockdown cells, to a single cell migration. The MYOF KD cells likely exhibit increased directionality and collective migration due to their increase in cell-cell adhesion, inhibiting their ability to migrate away from their neighbors. A switch back to decreased directionality after TGF-β1 treatment further confirms the occurrence of EMT, since the cells are able to more easily break away from their neighbors to migrate as a single cell. The representative images seen in Figure 4-7 further support the result that the TGF-β1 treated MYOF KD cells exhibit single cell migration, since many cells are seen migrating away from their neighbors. The vehicle-treated MYOF KD cells appear as a single wall of cells, moving together.

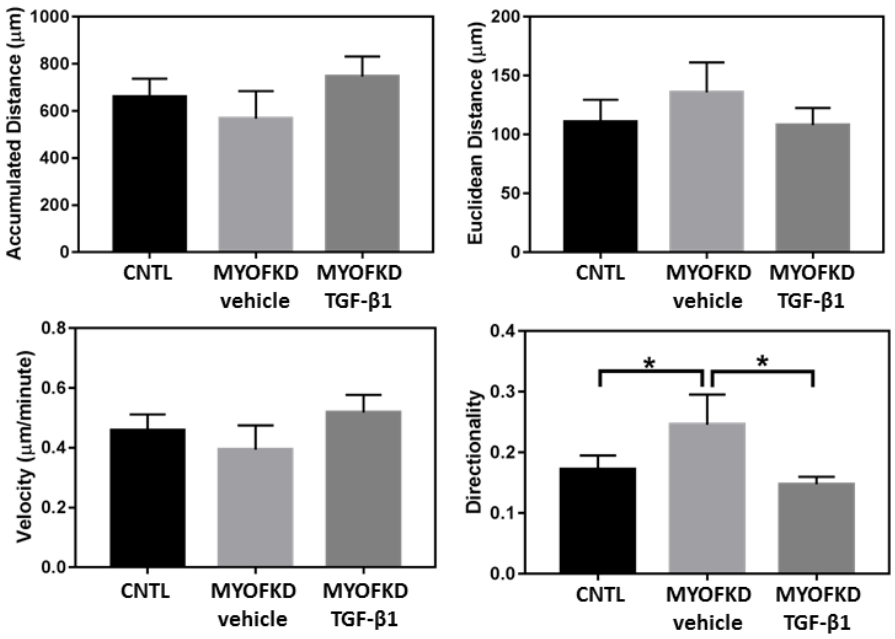

Figure 4-6: Migration of MDA-MB-231 Cells. Graphs of accumulated distance, Euclidean distance, velocity, and directionality from 24 hours of migration, presented here is the average values across all cells of each condition. The MYOF KD cells were found to have significantly greater directionality than both the CNTL and MYOF KD with TGF-β1. n=3+SD, *p<0.05

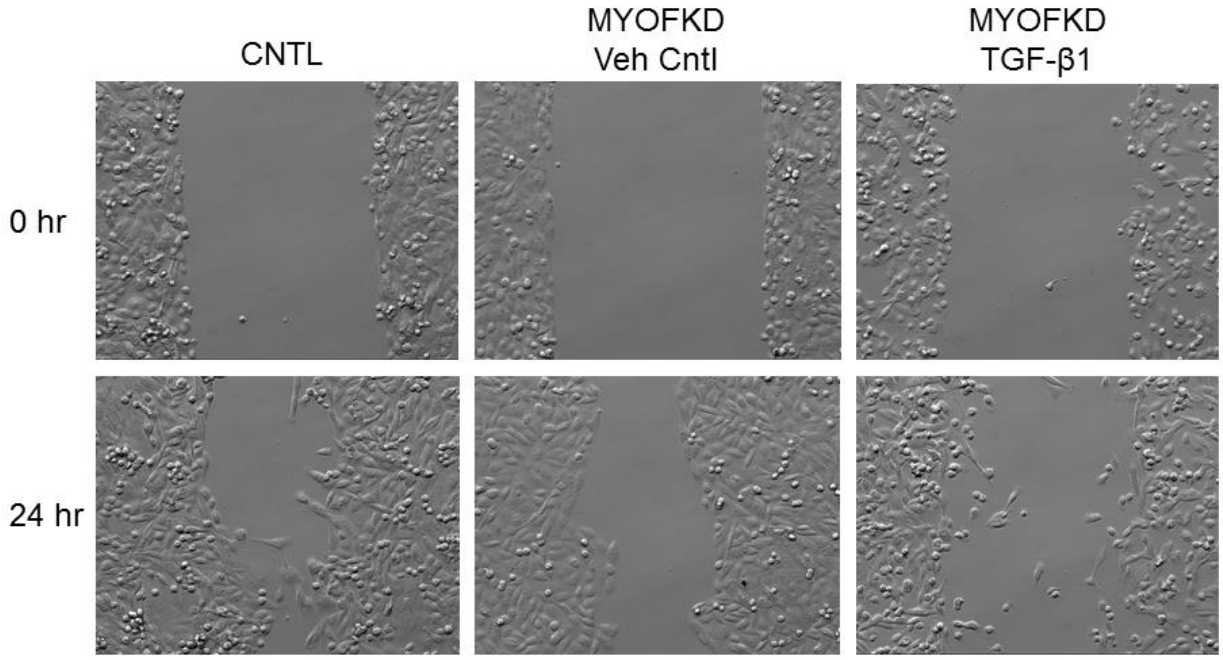

Figure 4-7: Phase Images Before and After Migration. Representative phase images of each condition before and after migration, showing the differences in the edge of the cells with each condition.

4.4 The Mechanical Environment and Matrix Metalloproteinase Activity of MDA-MB-231 Cells

Since EMT is associated with increased MMP activity, and as cancer progresses, the surrounding tissue stiffens, we sought to examine the relationship between MMP activity and mechanical environment, and how myoferlin depletion affects their interaction (Levental et al. 2009). To examine the effect of mechanical forces on the MMP activity of MDA-MB-231 control and MYOF KD cells, cells were encapsulated in PEG hydrogels of varying elastic modulus. Stiffness was varied by changing the molecular weight and number of arms of the PEG and varying the crosslinking ratio, as described above. MMP activity was measured using a fluorescent peptide sensitive to cleavage by MMP-14, and normalizing to the metabolic activity and DNA content. MMP activity was found to increase with increasing elastic modulus of the gel for both the control and MYOF KD cells, as shown in Figure 4-8. Using linear regression analysis, the control and MYOF KD cells were found to have the same slope, indicating they have the same response to stiffness. However, the y-intercepts of each regression were found to be significantly different, with a p-value of 0.0055. Thus, the control cells have higher MMP activity than the MYOF KD cells across conditions.

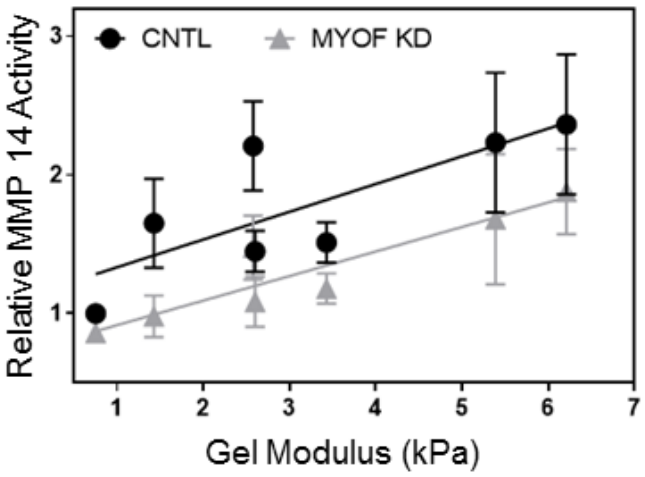

Figure 4-8: Effect of Gel Stiffness on MMP Activity of MDA-MB-231 Cells. Relationship between elastic modulus and MMP activity in the control and MYOF KD cells.

Chapter 5 Conclusions and Future Directions

5.1 Conclusions

EMT contributes to cancer progression and poor prognosis through either enhanced migration to form metastases or resistance to therapeutics. How EMT is regulated and ways to target this process is an area of importance in research, in order to develop new therapeutics and better understand the mechanism of disease. In this study, we have investigated the mechanism by which myoferlin depletion leads to the reversal of EMT, and whether this change is permanent.

In Chapter 4.1, we demonstrated that the MDA-MB-231 MYOF KD cells retain their ability to undergo EMT. Treatment with exogenous TGF-β1 led to a visible morphology change in the MYOF KD cells to a spindle-like shape characteristic of mesenchymal cells, which was accompanied by a phenotypic change with an increase in vimentin and decrease in E-cadherin expression. Thus, the mechanism of EMT remains intact in the MYOF KD cells.

The production of autocrine TGF-β1 by each cell type was explored in Chapter 4.2. Direct detection of TGF-β1 showed approximately a 20% decrease in production by the MYOF KD cells relative to the control cells. Similarly, mRNA expression of TGF-β1 showed a 30% decrease in the MYOF KD cells relative to the control, although this change was not found to be significant. These results indicate that TGF-β1 production could be responsible in part for the MET occurring after MYOF depletion.

Cell behavior including migration and MMP activity were investigated in Chapters 4.3 and 4.4. Migration studies found TGF-β1 treated MYOF KD cells to have decreased directionality to levels similar to that of the control cells, indicating a change to single cell migration. Elastic modulus of the 3D environment was shown to have a significant effect on the

MMP activity of both the control and MYOF KD cells, with increasing stiffness resulting in corresponding increasing MMP activity. MYOF KD cells were found to have significantly lower MMP activity than the control cells, reinforcing their phenotype change, since EMT is associated with increased MMP activity.

5.2 Future Directions

In this study, we have demonstrated that the MYOF KD cells are capable of undergoing a phenotypical change to become more mesenchymal, however, corresponding studies on changes in cell behavior are lacking. Ongoing studies to examine the invasion of the MYOF KD cells after TGF-β1 treatment are being conducted, and would strengthen the conclusion that the cells have undergone EMT by showing behavior characteristic of mesenchymal cells, and similar to the control cells. Studies on the effect of mechanical environment with the hydrogels could be expanded to examine the effects of TGF-β1 treatment on the MYOF KD MMP activity after EMT is observed, to determine if MMP activity increases to values similar to the control cells.

Since we have shown that TGF-β1 production is affected by MYOF depletion, blocking TGF-β in the control cells and observing MET would strengthen this connection. Ongoing studies in the lab have begun to examine this possibility using both a neutralizing antibody and a pharmacological inhibitor (data not shown). Issues arose with cell viability during the experiments, likely due to the need of MDA-MB-231 cells to have autocrine TGF-β for their growth and survival (Lei et al. 2002). Future studies could examine a dose dependent response, to determine if there is a critical amount of inhibition that can cause MET without severely inhibiting cell growth. Along with inducing MET, studies on cell behavior with inhibitors could be conducted as well to show a change to a more epithelial phenotype and activity. Similarly, treatment with TGF-β1 could also be examined with a dose response, to determine the

concentration of TGF-β1 necessary for EMT to occur in the MYOF KD cells. The concentration of TGF-β1 used for treatment (2ng/mL) was much higher than the concentrations found to be made by MDA-MB-231s (approximately 100-200 pg/mL).

Another possible direction would be to explore other proteins that myoferlin interacts with to potentially identify other mechanisms by which myoferlin depletion is leading to MET. One such protein recently discovered to be regulated by myoferlin is A Disintegrin and Metalloproteinase 12 (ADAM12), which is involved in cancer formation and progression by enhancing proliferation and invasion and is highly expressed in breast cancer. Myoferlin was found to enhance the stability and enzymatic activity of ADAM12, which would help lead to the reduction of its substrate, E-cadherin, a known EMT regulator (Zhou et al. 2016). ADAM12 has further been found to contribute to TGF-β induced EMT, further contributing to the possibility of its role in the present mechanism. However, inhibiting ADAM12 in MDA-MB-231 cells did not reverse their mesenchymal phenotype, indicating that ADAM12 alone is not inducing EMT (Ruff et al. 2015). Exploring the interaction of all three factors, myoferlin, TGF-β, and ADAM12, could be interesting and lead to new insight about the mechanism of myoferlin depletion in MDA-MB-231 cells. Furthermore, identifying other proteins that interact with myoferlin, either through literature review or bioinformatics analysis, could aid in the discovery of other potential targets that contribute to the MET seen with myoferlin depletion.

References

Bernatchez, Pascal N., Arpeeta Sharma, Pinar Kodaman, and William C. Sessa. 2009. "Myoferlin Is Critical for Endocytosis in Endothelial Cells." *American Journal of Physiology - Cell Physiology* 297 (3): C484–92. doi:10.1152/ajpcell.00498.2008.

Blackstone, B. N., R. Li, W. E. Ackerman, S. N. Ghadiali, H. M. Powell, and D. A. Kniss. 2015. "Myoferlin Depletion Elevates Focal Adhesion Kinase and Paxillin Phosphorylation and Enhances Cell-Matrix Adhesion in Breast Cancer Cells." *American Journal of Physiology. Cell Physiology* 308 (8): C642–49. doi:10.1152/ajpcell.00276.2014.

"Breast Cancer Facts & Figures | American Cancer Society." 2017. Accessed February 12. https://www.cancer.org/research/cancer-facts-statistics/breast-cancer-facts-figures.html.

Carman, Michelle L., Thomas G. Estes, Adam W. Feinberg, James F. Schumacher, Wade Wilkerson, Leslie H. Wilson, Maureen E. Callow, James A. Callow, and Anthony B. Brennan. 2006. "Engineered Antifouling Microtopographies--Correlating Wettability with Cell Attachment." *Biofouling* 22 (1-2): 11–21. doi:10.1080/08927010500484854.

Craene, Bram De, and Geert Berx. 2013. "Regulatory Networks Defining EMT during Cancer Initiation and Progression." *Nature Reviews Cancer* 13 (2): 97–110. doi:10.1038/nrc3447.

Davies, J. A. 1996. "Mesenchyme to Epithelium Transition during Development of the Mammalian Kidney Tubule." *Acta Anatomica* 156 (3): 187–201.

Dhasarathy, Archana, Masahiro Kajita, and Paul A. Wade. 2007. "The Transcription Factor Snail Mediates Epithelial to Mesenchymal Transitions by Repression of Estrogen Receptor-A." *Molecular Endocrinology* 21 (12): 2907–18. doi:10.1210/me.2007-0293.

Elias, Maria C, Kathleen R Tozer, John R Silber, Svetlana Mikheeva, Mei Deng, Richard S Morrison, Thomas C Manning, et al. 2005. “TWIST Is Expressed in Human Gliomas and Promotes Invasion.” *Neoplasia (New York, N.Y.)* 7 (9): 824–37.

Evans, Andrew, Patsy Whelehan, Kim Thomson, Denis McLean, Katrin Brauer, Colin Purdie, Lee Baker, Lee Jordan, Petra Rauchhaus, and Alastair Thompson. 2012. “Invasive Breast Cancer: Relationship between Shear-Wave Elastographic Findings and Histologic Prognostic Factors.” *Radiology* 263 (3): 673–77. doi:10.1148/radiol.12111317.

Fahmy, Karim, Arnaud Gonzalez, Mohammad Arafa, Paul Peixoto, Akeila Bellahcène, Andrei Turtoi, Philippe Delvenne, Marc Thiry, Vincent Castronovo, and Olivier Peulen. 2016. “Myoferlin Plays a Key Role in VEGFA Secretion and Impacts Tumor-Associated Angiogenesis in Human Pancreas Cancer.” *International Journal of Cancer* 138 (3): 652–63. doi:10.1002/ijc.29820.

Fischer, Kari R., Anna Durrans, Sharrell Lee, Jianting Sheng, Fuhai Li, Stephen T. C. Wong, Hyejin Choi, et al. 2015. “Epithelial-to-Mesenchymal Transition Is Not Required for Lung Metastasis but Contributes to Chemoresistance.” *Nature* 527 (7579): 472–76. doi:10.1038/nature15748.

Ganapathy, Vidya, Rongrong Ge, Alison Grazioli, Wen Xie, Whitney Banach-Petrosky, Yibin Kang, Scott Lonning, et al. 2010. “Targeting the Transforming Growth Factor-Beta Pathway Inhibits Human Basal-like Breast Cancer Metastasis.” *Molecular Cancer* 9 (May): 122. doi:10.1186/1476-4598-9-122.

Gomes, Luciana R., Letícia F. Terra, Rosângela AM Wailemann, Leticia Labriola, and Mari C. Sogayar. 2012. “TGF-β1 Modulates the Homeostasis between MMPs and MMP

Inhibitors through p38 MAPK and ERK1/2 in Highly Invasive Breast Cancer Cells." *BMC Cancer* 12: 26. doi:10.1186/1471-2407-12-26.

Guilford, P., J. Hopkins, J. Harraway, M. McLeod, N. McLeod, P. Harawira, H. Taite, R. Scoular, A. Miller, and A. E. Reeve. 1998. "E-Cadherin Germline Mutations in Familial Gastric Cancer." *Nature* 392 (6674): 402–5. doi:10.1038/32918.

Hugo, Honor, M. Leigh Ackland, Tony Blick, Mitchell G. Lawrence, Judith A. Clements, Elizabeth D. Williams, and Erik W. Thompson. 2007. "Epithelial—mesenchymal and Mesenchymal—epithelial Transitions in Carcinoma Progression." *Journal of Cellular Physiology* 213 (2): 374–83. doi:10.1002/jcp.21223.

Itoh, Yoshifumi. 2015. "Membrane-Type Matrix Metalloproteinases: Their Functions and Regulations." *Matrix Biology: Journal of the International Society for Matrix Biology* 44-46 (July): 207–23. doi:10.1016/j.matbio.2015.03.004.

Janda, Elzbieta, Kerstin Lehmann, Iris Killisch, Martin Jechlinger, Michaela Herzig, Julian Downward, Hartmut Beug, and Stefan Grünert. 2002. "Ras and TGF[beta] Cooperatively Regulate Epithelial Cell Plasticity and Metastasis: Dissection of Ras Signaling Pathways." *The Journal of Cell Biology* 156 (2): 299–313. doi:10.1083/jcb.200109037.

Kalluri, Raghu, and Robert A. Weinberg. 2009. "The Basics of Epithelial-Mesenchymal Transition." *The Journal of Clinical Investigation* 119 (6): 1420–28. doi:10.1172/JCI39104.

Katsuno, Yoko, Samy Lamouille, and Rik Derynck. 2013. "TGF-B Signaling and Epithelial-Mesenchymal Transition in Cancer Progression." *Current Opinion in Oncology* 25 (1): 76–84. doi:10.1097/CCO.0b013e32835b6371.

Kim, Nam Hee, Hyun Sil Kim, Xiao-Yan Li, Inhan Lee, Hyung-Seok Choi, Shi Eun Kang, So Young Cha, et al. 2011. “A p53/miRNA-34 Axis Regulates Snail1-Dependent Cancer Cell Epithelial–mesenchymal Transition.” *The Journal of Cell Biology* 195 (3): 417–33. doi:10.1083/jcb.201103097.

Korpal, Manav, Esther S. Lee, Guohong Hu, and Yibin Kang. 2008. “The miR-200 Family Inhibits Epithelial-Mesenchymal Transition and Cancer Cell Migration by Direct Targeting of E-Cadherin Transcriptional Repressors ZEB1 and ZEB2.” *The Journal of Biological Chemistry* 283 (22): 14910–14. doi:10.1074/jbc.C800074200.

Leight, Jennifer L., Daniel L. Alge, Andrew J. Maier, and Kristi S. Anseth. 2013. “Direct Measurement of Matrix Metalloproteinase Activity in 3D Cellular Microenvironments Using a Fluorogenic Peptide Substrate.” *Biomaterials* 34 (30): 7344–52. doi:10.1016/j.biomaterials.2013.06.023.

Leight, Jennifer L., Michele A. Wozniak, Sophia Chen, Michelle L. Lynch, and Christopher S. Chen. 2012. “Matrix Rigidity Regulates a Switch between TGF-β1-Induced Apoptosis and Epithelial-Mesenchymal Transition.” *Molecular Biology of the Cell* 23 (5): 781–91. doi:10.1091/mbc.E11-06-0537.

Lei, Xiufen, Abhik Bandyopadhyay, Thy Le, and LuZhe Sun. 2002. “Autocrine TGFbeta Supports Growth and Survival of Human Breast Cancer MDA-MB-231 Cells.” *Oncogene* 21 (49): 7514–23. doi:10.1038/sj.onc.1205966.

Leung, Cleo, Carol Yu, Michelle I. Lin, Cristina Tognon, and Pascal Bernatchez. 2013. “Expression of Myoferlin in Human and Murine Carcinoma Tumors: Role in Membrane Repair, Cell Proliferation, and Tumorigenesis.” *The American Journal of Pathology* 182 (5): 1900–1909. doi:10.1016/j.ajpath.2013.01.041.

Levental, Kandice R., Hongmei Yu, Laura Kass, Johnathon N. Lakins, Mikala Egeblad, Janine T. Erler, Sheri F. T. Fong, et al. 2009. “Matrix Crosslinking Forces Tumor Progression by Enhancing Integrin Signaling.” *Cell* 139 (5): 891–906. doi:10.1016/j.cell.2009.10.027.

Li, Ruth, William E. Ackerman, Cosmin Mihai, Leonithas I. Volakis, Samir Ghadiali, and Douglas A. Kniss. 2012. “Myoferlin Depletion in Breast Cancer Cells Promotes Mesenchymal to Epithelial Shape Change and Stalls Invasion.” *PloS One* 7 (6): e39766. doi:10.1371/journal.pone.0039766.

Liu, Jieqiong, Shan Liao, Benjamin Diop-Frimpong, Wei Chen, Shom Goel, Kamila Naxerova, Marek Ancukiewicz, Yves Boucher, Rakesh K. Jain, and Lei Xu. 2012. “TGF-B Blockade Improves the Distribution and Efficacy of Therapeutics in Breast Carcinoma by Normalizing the Tumor Stroma.” *Proceedings of the National Academy of Sciences* 109 (41): 16618–23. doi:10.1073/pnas.1117610109.

Martin, Tracey A., Amit Goyal, Gareth Watkins, and Wen G. Jiang. 2005. “Expression of the Transcription Factors Snail, Slug, and Twist and Their Clinical Significance in Human Breast Cancer.” *Annals of Surgical Oncology* 12 (6): 488–96. doi:10.1245/ASO.2005.04.010.

Medici, Damian, Elizabeth D. Hay, and Bjorn R. Olsen. 2008. “Snail and Slug Promote Epithelial-Mesenchymal Transition through B-Catenin–T-Cell Factor-4-Dependent Expression of Transforming Growth Factor-β3.” *Molecular Biology of the Cell* 19 (11): 4875–87. doi:10.1091/mbc.E08-05-0506.

Moustakas, Aristidis, and Carl-Henrik Heldin. 2016. “Mechanisms of TGFβ-Induced Epithelial–Mesenchymal Transition.” *Journal of Clinical Medicine* 5 (7). doi:10.3390/jcm5070063.

Nyga, Agata, Umber Cheema, and Marilena Loizidou. 2011. “3D Tumour Models: Novel in Vitro Approaches to Cancer Studies.” *Journal of Cell Communication and Signaling* 5 (3): 239. doi:10.1007/s12079-011-0132-4.

Paszek, Matthew J., Nastaran Zahir, Kandice R. Johnson, Johnathon N. Lakins, Gabriela I. Rozenberg, Amit Gefen, Cynthia A. Reinhart-King, et al. 2005. “Tensional Homeostasis and the Malignant Phenotype.” *Cancer Cell* 8 (3): 241–54. doi:10.1016/j.ccr.2005.08.010.

Perentes, Jean Y., Nathaniel D. Kirkpatrick, Satoshi Nagano, Eve Y. Smith, Christine M. Shaver, Dennis Sgroi, Igor Garkavtsev, Lance L. Munn, Rakesh K. Jain, and Yves Boucher. 2011. “Cancer Cell–Associated MT1-MMP Promotes Blood Vessel Invasion and Distant Metastasis in Triple-Negative Mammary Tumors.” *Cancer Research* 71 (13): 4527–38. doi:10.1158/0008-5472.CAN-10-4376.

Ruff, Michaël, Anthony Leyme, Fabienne Le Cann, Dominique Bonnier, Jacques Le Seyec, Franck Chesnel, Laurent Fattet, Ruth Rimokh, Georges Baffet, and Nathalie Théret. 2015. “The Disintegrin and Metalloprotease ADAM12 Is Associated with TGF-B-Induced Epithelial to Mesenchymal Transition.” *PloS One* 10 (9): e0139179. doi:10.1371/journal.pone.0139179.

Têtu, Bernard, Jacques Brisson, Chang Shu Wang, Hélène Lapointe, Geneviève Beaudry, Caty Blanchette, and Dominique Trudel. 2006. “The Influence of MMP-14, TIMP-2 and MMP-2 Expression on Breast Cancer Prognosis.” *Breast Cancer Research: BCR* 8 (3): R28. doi:10.1186/bcr1503.

Volakis, Leonithas I., Ruth Li, William E. Ackerman, Cosmin Mihai, Meagan Bechel, Taryn L. Summerfield, Christopher S. Ahn, et al. 2014. “Loss of Myoferlin Redirects Breast

Cancer Cell Motility towards Collective Migration." *PloS One* 9 (2): e86110. doi:10.1371/journal.pone.0086110.

Wu, Mary Y., and Caroline S. Hill. 2009. "TGF-B Superfamily Signaling in Embryonic Development and Homeostasis." *Developmental Cell* 16 (3): 329–43. doi:10.1016/j.devcel.2009.02.012.

Yang, Jing, and Robert A. Weinberg. 2008. "Epithelial-Mesenchymal Transition: At the Crossroads of Development and Tumor Metastasis." *Developmental Cell* 14 (6): 818–29. doi:10.1016/j.devcel.2008.05.009.

Yin, Kai, Wenjin Yin, Yaohui Wang, Liheng Zhou, Yu Liu, Gong Yang, Jianhua Wang, and Jinsong Lu. 2016. "MiR-206 Suppresses Epithelial Mesenchymal Transition by Targeting TGF-B Signaling in Estrogen Receptor Positive Breast Cancer Cells." *Oncotarget* 7 (17): 24537–48. doi:10.18632/oncotarget.8233.

Zheng, Xiaofeng, Julienne L. Carstens, Jiha Kim, Matthew Scheible, Judith Kaye, Hikaru Sugimoto, Chia-Chin Wu, Valerie S. LeBleu, and Raghu Kalluri. 2015. "Epithelial-to-Mesenchymal Transition Is Dispensable for Metastasis but Induces Chemoresistance in Pancreatic Cancer." *Nature* 527 (7579): 525–30. doi:10.1038/nature16064.

Zhou, Yanqing, Lipeng Xiong, Yang Zhang, Rong Yu, Xiaogang Jiang, and Guoqiang Xu. 2016. "Quantitative Proteomics Identifies Myoferlin as a Novel Regulator of A Disintegrin and Metalloproteinase 12 in HeLa Cells." *Journal of Proteomics* 148 (October): 94–104. doi:10.1016/j.jprot.2016.07.015.

Appendix A: MATLAB Code

```
clear all
files=dir('*KD_Control*.xls');
cnt=1;
for i=1:size(files)
    A=dlmread(files(i).name,'\t',1,0);
    cell_count=A(length(A),2);
    for j=1:cell_count
        B=A(A(:,2)==j,2:5);
        for k=2:length(B)
            Dist(k-1)=sqrt(((B(k,3)-B((k-1),3))*(1/1.55))^2+((B(k,4)-B((k-
1),4))*(1/1.55))^2);
        end
        Acc_dist(cnt)=sum(Dist);
        Velocity(cnt)=mean(Dist)/10;
        Euc_dist(cnt)=sqrt(((B(end,3)-B(1,3))*(1/1.55))^2+((B(end,4)-
B(1,4))*(1/1.55))^2);
        Directionality(cnt)=Euc_dist(cnt)/Acc_dist(cnt);
        cnt=cnt+1;
    end
end
filename=sprintf('%s_Analysis.xls',files(1).name(end-19:end-4));
xlswrite(filename,[Acc_dist',Velocity',Euc_dist',Directionality']);
```

Appendix B: Cell Proliferation and Metabolism

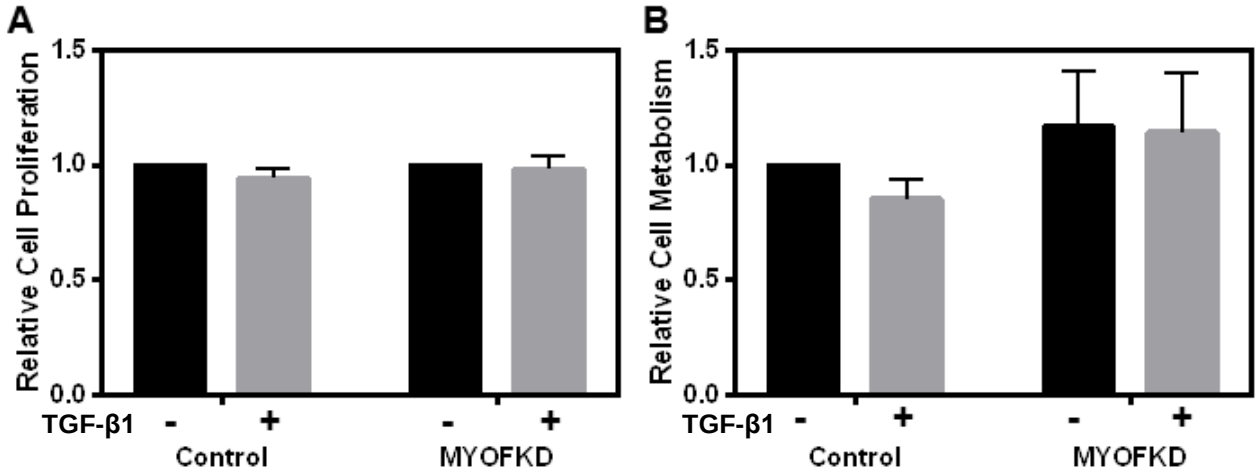

Figure B-1: Effect of TGF-β1 on Proliferation and Metabolism. A.) Cells were cultured +/- TGF-β1 for 48 hours. Relative cell proliferation was determined using the CyQUANT kit according to the manufacturer's instructions. Values were normalized to the control treated condition for each cell type. Statistical analysis using a two-way ANOVA with a Tukey's multiple comparison test found no significant differences in the data set. n=3 B.) Cells were cultured +/- TGF-β1 for 48 hours. Cell metabolism was determined using the AlamarBlue cell viability reagent. Values were normalized to the control cells vehicle treatment. A two-way ANOVA with Tukey's multiple comparison test was used to determine significance, and no significant differences were found within the data set. n=3